Phosphorus removal and recovery from wastewater using Fe-dosing bioreactor and co-fermentation: Investigation by X-ray absorption near edge structure (XANES) spectroscopy

Ruo-hong Li[†,§], Jin-li Cui[‡,⊥], Xiang-dong Li[‡], Xiao-yan Li[*,†,§,‖]

[†]Environmental Engineering Research Centre, Department of Civil Engineering, The University of Hong Kong, Pokfulam, Hong Kong, China

[‡]Department of Civil and Environmental Engineering, The Hong Kong Polytechnic University, Hung Hom, Kowloon, Hong Kong, China

[§]Shenzhen Engineering Research Laboratory for Sludge and Food Waste Treatment and Resource Recovery, Graduate School at Shenzhen, Tsinghua University, Shenzhen, China

[‖]Tsinghua-Berkeley Shenzhen Institute, Tsinghua University, Shenzhen, China

[⊥]Key Laboratory for Water Quality and Conservation of the Pearl River Delta, Ministry of Education; School of Environmental Science and Engineering, Guangzhou University, Guangzhou, China

(*Corresponding author: phone: 852-28592659; fax: 852-28595337; E-mail: xlia@hku.hk)

Abstract

A new phosphorus (P) removal and recovery process that integrates an $FeCl_3$-dosing, membrane bioreactor (MBR) and side-stream co-fermentation was developed for wastewater treatment. The Fe and P species and their transformation mechanisms via aerobic and anaerobic conditions were investigated with X-ray absorption near edge structure (XANES) spectroscopy. In the new treatment system, 98.4% of the total P in domestic wastewater was removed and retained in activated sludge in the MBR. During the subsequent acidogenic co-fermentation with food waste, P in the MBR sludge was released and eventually recovered as vivianite, achieving an overall P recovery efficiency of 61.9% from wastewater. The main pathways for

P removal and recovery with iron (Fe) dosing and acidogenic fermentation were determined by XANES analysis. The results showed that Fe-enhanced P removal with the MBR was mainly achieved by precipitation as ferric phosphate (24.2%) and adsorption onto hydrous iron oxides (60.3%). During anaerobic fermentation, transition from Fe(III)-P to Fe(II)-P complex occurred in the sludge, leading to Fe(II) dissolution and P release. The pH decrease and microbial Fe reduction were crucial conditions for effective P extraction from the MBR sludge. The efficiency of P recovery increased with an increase in the fermentation time and organic load and a decrease of pH in the solution.

Abstract Graphic

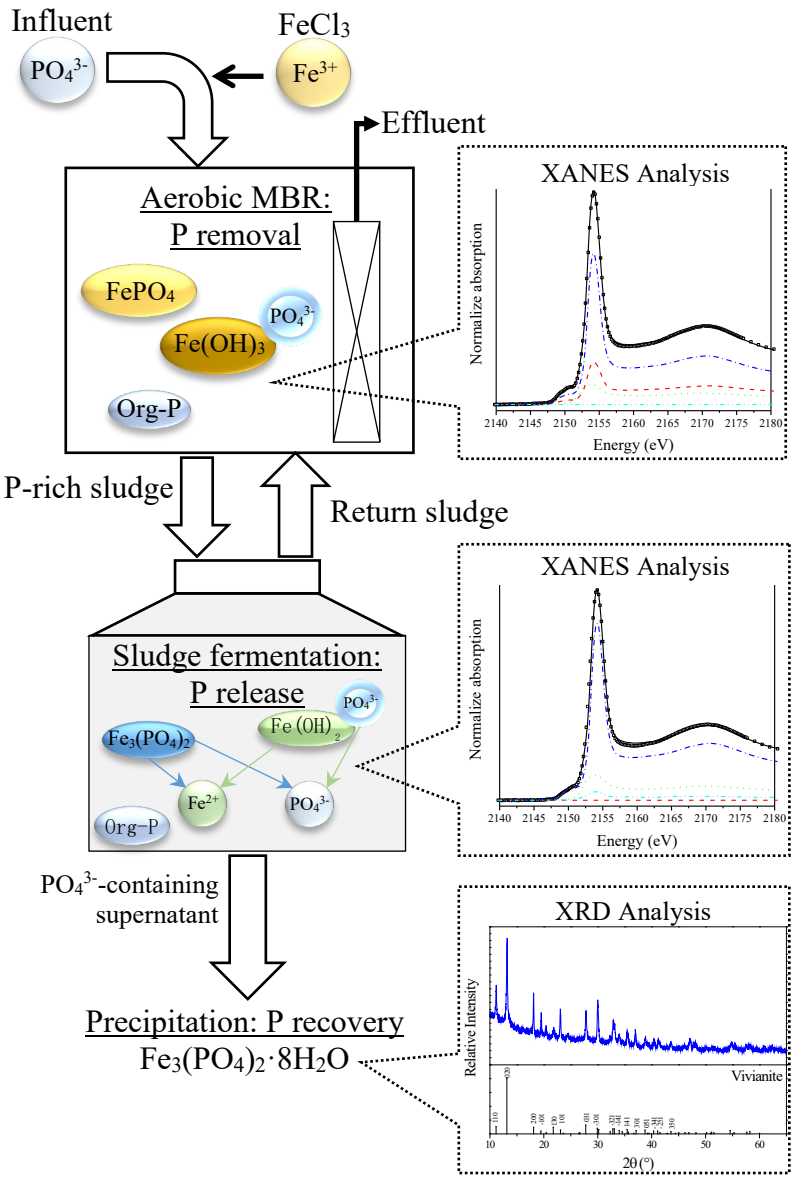

1. Introduction

Membrane bioreactor (MBR) technology has increasingly been used for biological wastewater treatment and reuse, owing to advantages such as a small footprint, high organic loading rate, and excellent effluent quality. However, the typical MBR process performs poorly in phosphorus (P) removal. Phosphorus is one of the principal nutrient elements in water bodies

and is responsible for eutrophication and related surface water quality problems. To remove phosphorus from wastewater, MBRs may be used in combination with the chemical phosphorus removal (CPR) process.[1, 2] CPR has been widely applied in wastewater treatment for effective and stable P removal. In this process, metal salts are dosed into wastewater to form P-incorporated solids, and ferric chloride ($FeCl_3$) is the most common chemical used for CPR.[3] Iron dosing into the MBR influent could lower the total phosphorus (TP) concentration in the effluent to below 0.5 mg/L.[1, 2]

Phosphorus is also a valuable and non-substitutable resource for agricultural production. The rapid depletion of natural P reserves will greatly threaten global food security.[4] It is thus urgent to recover and recycle P from all possible sources, including wastewater and sludge. The German cabinet recently passed a sewage sludge ordinance that requires all large wastewater treatment plants in Germany to recover P from sewage sludge.[5] Existing P removal and recovery processes adopt either biological or chemical approaches. Phosphorous removal from wastewater can be achieved by the enhanced biological P removal (EBPR) process. However, EBPR heavily relies on the proliferation of polyphosphate-accumulating organisms (PAOs) which is difficult to achieve and maintain in full scale applications.[3] In comparison, chemical precipitation is more effective and reliable for enhanced P removal from wastewater. Upon sufficient P removal and adequate concentration into the sludge, anaerobic digestion can be applied to hydrolyzed various forms of phosphorous into orthophosphate for possible P recovery.[6] However, the fraction of P release into the liquid phase of the sludge is rather limited during the sludge digestion. The most common method to recover P from waste sludge or sludge ash is chemical acidification extraction, such as the Stuttgart process[7] and RecoPhos[8]. However, this method uses a large amount of strong acids, which not only increases the operating difficulty and cost, but also gives rise to a serious problem of secondary pollution.[9] These drawbacks have considerably hindered the practical application of P recovery from

wastewater and sludge.

In a recent study, we developed an integrated chemical-biological process for P removal and recovery during municipal wastewater treatment processes.[10, 11] The new treatment system consisted of an Fe-dosing CPR together with an aerobic MBR for enhanced P removal and side-stream acidogenic sludge fermentation for P recovery from the P-rich MBR sludge. The process was designed to make use of the transformation from ferric iron (Fe(III)) to ferrous iron (Fe(II)) under an anaerobic condition, in addition to the substantially different solubility between the Fe(III)-based and Fe(II)-based chemical compounds, to extract P from the sludge for recovery. Compared with chemical acidification extraction, the biological sludge acidogenesis method for P extraction from Fe-loaded sludge is not only more environmentally friendly but also preserves the activity of the biomass sludge.

However, the presence of Fe is usually considered as a negative factor when evaluating P recovery options.[12] It was actually found from the previous tests that P release from the sludge could not be fully achieved, which would affect the overall P recovery efficiency.[11] The transformations of the Fe and P species throughout the aerobic and anaerobic phases of the systems are complicated. For Fe-enhanced CPR, ferric iron and phosphate in the sludge mixture can react to the precipitation of ferric phosphate ($FePO_4$). In addition, Fe(III) may also form hydrous iron oxide (HFO) precipitates, such as ferrihydrite ($Fe(OH)_3$) and goethite (α-FeOOH), onto which phosphate is adsorbed.[13] Theoretically, one mole of ferric iron can precipitate one mole of phosphorus to form $FePO_4$. In reality, the optimal Fe/P molar ratio is usually higher than the $FePO_4$ stoichiometry, due to the hydrolysis of iron.[14] Hauduc and co-workers[15] suggested that P adsorption onto HFO is the more dominant reaction for CPR. Moreover, the Fe and P speciation in the aerobic MBR with a long sludge retention time (SRT) can be more complex than that of the simple CPR, considering the long duration for chemical transitions. Information is particularly scarce about the transformation of iron and phosphorus species in

the sludge in dynamic aerobic and anaerobic reactors of the systems, and the main pathways and mechanisms of P removal and recovery during the chemical-biological treatment process requires further clarification.

The traditional speciation analysis of Fe and P compounds in a solid sample was mainly achieved by chemical extraction techniques.[16, 17] These methods can only provide rough information and unrefined results due to species variations during the multi-step chemical treatment of the sample. X-ray absorption spectroscopy (XAS) is a powerful technology for determination of chemical speciation and relative species fractions in a complicated mixture. XAS has been extensively used to characterize or identify the structural details of trace elements in environmental samples[18] and to quantify mineral composition in sludge.[19] In this study, the objective was to investigate the quantitative P and Fe speciation in aerobic MBR and anaerobic fermenters using X-ray absorption near edge structure (XANES) spectroscopy at both Fe and P K-edges. The Fe and P species and their relative abundances were determined at different stages of wastewater treatment and sludge processing. The findings regarding the transitions of Fe and P in the sludge under different conditions can provide new insights into the pathways and controlling factors for effective P removal and recovery in the chemical-biological wastewater treatment system.

2. Materials and Methods

2.1 Fe-dosing MBR and sludge acidogenesis system for enhanced P removal and recovery

A new chemical-biological process was developed for efficient P removal and recovery in municipal wastewater treatment. As shown in Figure 1, the process involved three main steps. (1) Reliable P removal by the CPR together with an aerobic MBR: $FeCl_3$-based chemical precipitation and flocculation was applied to the wastewater influent before the MBR to form

Fe(III)-P complex and retain P in the sludge suspension of the MBR. (2) Biological P extraction from the MBR sludge: effective P release from the sludge was achieved by acidogenic fermentation in a side-stream. Dissimilatory iron reduction during sludge fermentation led to iron dissolution, releasing P into the liquid phase of the sludge. Low-cost organic wastes, such as food wastes, were added for co-fermentation to enhance the production of volatile fatty acids (VFAs) and hence lower the solution pH.[20] Unlike chemical acidification of the sludge for P recovery, biological acidogenesis lowered the sludge pH to dissolve P without deactivating the biomass. Thus, the settled sludge was returned to the aerobic MBR to retain its long sludge retention time (SRT) for wastewater treatment. (3) Phosphorus recovery: with simple pH neutralization, P was readily recovered by re-precipitation from the supernatant of the fermented sludge.

2.2 Experimental details

The experimental system with an aerobic MBR and anaerobic fermenters was continuously operated to treat raw domestic sewage collected from a local treatment plant (Stanley Sewage Treatment Works, Hong Kong). A summary of the major configurational and operational parameters of the experimental system is given in Table S1 of Supporting Information (SI). The wastewater was pre-flocculated by $FeCl_3$ (20 mg-Fe/L) without sedimentation before pumping into the MBR tank. A flat-plate ceramic membrane module with an effective surface area of 0.0384 m^2 and an average pore size of 100 nm (Meidensha Corporation, Japan) was submerged in the tank to form the MBR with a working volume of 8 L. The MBR was filled with activated sludge that had a suspended solids (SS) concentration of around 4.2 g/L. Aeration was supplied from the bottom of the MBR to keep the dissolved oxygen (DO) concentration greater than 4 mg/L. A suction pump (Master FLEX, Cole-Parmer) was used to withdraw effluent from the MBR following an intermittent filtration mode with 5

142 h 55 min filtration and 5 min backwash in each operating cycle (4 cycles/d). The MBR had a
143 filtration flux of 17.4 L/h-m^2 (LHM), a backwashing flux of 46.9 LHM, and an overall
144 hydraulic retention time (HRT) of 12 h. The trans-membrane pressure (TMP) was monitored
145 during the MBR operation.

146 The activated sludge suspension from the aerobic MBR was recirculated at a
147 predetermined rate through the anaerobic reactors, or fermenters, in side-stream for P
148 extraction and recovery. Cooked rice, as a model starch-rich food waste, was also added into
149 the fermenters to enhance the sludge acidogenesis and P release. Three fermenters with a
150 working volume of 1.76 L each were used to receive the sludge from the MBR on alternative
151 days. Each day, 1.6 L MBR sludge suspension, 160 mL of the residual seed sludge together
152 with the cooked rice slurry (organic loading rate of 2 g chemical oxygen demand (COD)/L)
153 was fed into one fermenter. After 72 h of fermentation with magnetic stirring at room
154 temperature, 1.6 L of the sludge suspension was withdrawn, and the remaining 160 mL of
155 sludge was reserved as the seed in the fermenter for the next batch of fermentation. The 1.6 L
156 of fermented sludge mixture was allowed to settle for 30 min; 1 L of supernatant was then
157 collected for P recovery. Of the settled sludge, 500 mL was returned to the aerobic MBR and
158 100 mL was discarded as waste sludge, resulting in an SRT of about 30 d for the aerobic MBR.

159 To recover P from the supernatant, the solution pH was adjusted to 8.0 by adding 2-M
160 NaOH, followed by stirring for 30 min. Under such conditions, orthophosphate in the
161 supernatant precipitated with ferrous iron to form iron phosphate complex. The mixture was
162 then centrifuged for 1 min for solid-liquid separation. The precipitates that contained P were
163 dried and analyzed for P species and the overall P recovery efficiency.

164

165 **2.3 Preparation and storage of the sludge samples for XANES analysis**

166 The activated sludge was sampled from the aerobic MBR tank after 90-day's stable

operation. The sludge was withdrawn from the MBR and fed into five anaerobic fermenters for batch fermentation. To investigate the effects of various factors (i.e., organic addition, pH, and fermentation time) on the transition of Fe and P throughout the fermentation process, the fermenters were operated under different conditions and sludge samples were collected after different periods, as summarized in Table 1. Reactor I was operated with the organic (food waste) loading but without pH control, and the anaerobic sludge samples were collected at different fermentation times from 0 to 72 h. Reactors II to V were operated with the organic loading and pH control at 3, 4, 5 and 6, and the anaerobic sludge samples were collected at the end of fermentation of 72 h. Reactor VI was the control reactor without food waste addition and pH control. The sludge samples were centrifuged at 6000 rpm for 15 min, and the dewatered solids were stored at -20°C for 4 h and then freeze-dried for 24 h. The sludge powder samples were placed in glass tubes filled with N_2 and stored at -20°C before XANES analysis.

2.4 X-ray absorption near edge structure spectroscopy for P and Fe speciation

P and Fe speciation in the different sludge samples was measured by an XAS on beamline 16A1 at the National Synchrotron Radiation Research Center (NSRRC), Taiwan. The sludge powder samples were pressed into pellets 5 mm in diameter and 1 to 2 mm in thickness, which were immediately posted on Kapton tape before measurement. The P and Fe speciation was determined by P K-edge (2145.5 eV) and Fe K-edge (7112.0 eV), respectively using a Si(111) double-crystal monochromator. The X-ray energy was calibrated by measuring the L_{III}-edge of Nb foil for P with E_0 at 2153.4 eV and Fe metal foil for Fe with E_0 at 7124.6 eV. The measurement was performed in fluorescence mode using an ionization chamber filled with helium gas (for I_0) and a Lytle detector filled with nitrogen gas (for I_f) under the ambient temperature and pressure.

Representative iron and phosphorus reference compounds that might exist in the aerobic

192 and anaerobic sludge were either obtained from chemical supplier (Sigma-Aldrich), or
193 synthesized according to the reference cited. Several compounds were considered in this study
194 for possible P and Fe species, including 2-line ferrihydrite ($Fe(OH)_3$)[21], goethite (α-FeOOH)[21],
195 akaganeite (β-FeOOH)[21], lepidocrocite (γ-FeOOH)[22], magnetite (Fe_3O_4), amorphous ferric
196 phosphate ($FePO_4$)[23], strengite ($FePO_4 \cdot 2H_2O$), vivianite ($Fe_3(PO_4)_2 \cdot 8H_2O$)[24], phosphate
197 adsorbed on hydrous ferric oxides (HFO)[25], phytic acid sodium salt hydrate
198 ($C_6H_{18}O_{24}P_6 \cdot xNa^+ \cdot yH_2O$), hydroxyapatite ($Ca_5(OH)(PO_4)_3$), newberyite ($MgHPO_4 \cdot 3H_2O$),
199 $Na_2HPO_4 \cdot 12H_2O$ and melanterite ($FeSO_4 \cdot 7H_2O$).

200 All collected spectra were processed with the Athena program.[26] The spectra of the ten
201 sludge samples were analyzed by principal component analysis (PCA)[27] using the SIXPACK
202 code[28] to determine the maximum number of components required to reproduce the XAS
203 spectra. Based on the PCA results, target transformation (TT) was further performed in order
204 to select appropriate reference compounds that are most likely present in the samples.[19, 29]
205 Based on the PCA/TT results, linear combination fitting (LCF) analysis in Athena was applied
206 to the XAS data to identify and quantify the species composition of the sludge samples.
207

208 **2.5 Analytical methods**

209 All samples were analyzed in triplicate, and the results reported are the mean values of the
210 measurements. The concentrations of COD, total nitrogen (TN), soluble orthophosphate (SP),
211 TP, soluble ferrous iron (SFe(II)), total iron (TFe), SS, and volatile suspended solids (VSS)
212 were determined according to Standard Methods.[30] For determination of soluble chemical
213 concentrations in a mixture, the samples were filtered through a 0.45-μm syringe PVDF
214 membrane (Millipore) before the measurement. A pH meter (Starter 2100, OHAUS) was used
215 to measure the solution pH. The DO concentration was measured with a digital DO meter (HI
216 2030, HANNA), and the oxidation-reduction potential (ORP) was detected with an ORP-meter

(HI 98201, HANNA).

VFAs, including acetic acid, propionic acid, butyric acid, isobutyric acid, valeric acid, isovaleric acid, isocaproic acid, caproic acid, and hexanoic acid, were quantified by gas chromatography (GC, Agilent 6890) equipped with a capillary column (Agilent 19095F-123) and a flame ionization detector (FID), following the procedure previously described.[11]

The fraction of Fe contents in the sludge samples was determined following the method described by Wang and Waite[31], including the total Fe(II) and Fe(III), and soluble Fe(II) and Fe(III). Accordingly, the fractions of insoluble Fe(II) and Fe(III) in the samples were calculated.

The X-ray powder diffraction (XRD) patterns of the sludge samples were obtained using a D8 advanced diffractometer (Bruker AXS, Karlsruhe, Germany) with a Cu Kα X-ray tube and a Lynxeye detector. XRD was used to identify the main crystalline compounds in the samples. The sludge samples were freeze-dried overnight and ground into powder before measurement. The analysis of the XRD data was performed using TOPAS 4.2 software (Bruker AXS GmbH, Germany).

3. Results

3.1 P removal and recovery from wastewater

3.1.1 P removal by the MBR with iron dosing

During the experimental study, the influent TP concentration was around 5.4 mg/L. For the Fe(III) dosing of 20 mg-Fe/L, the molar Fe/P ratio in the influent was about 2.04. The $FeCl_3$ addition helped achieve a final TP concentration below 0.1 mg/L in the effluent for 63.9% of the period and below 0.25 mg/L for 94.4% of the period. The average TP concentration in the effluent was about 0.1 mg/L. More than 98% of TP in the wastewater influent was retained as Fe(III)-P complex with the sludge suspension in the MBR tank.

241 3.1.2 P recovery from the MBR sludge by acidogenic co-fermentation

242 During stable operation of the system, the TP concentration in the MBR sludge was around
243 110.0 mg/L. After 3 d of fermentation in the fermenters, around 48.9% of TP was released
244 from the sludge as orthophosphate into the liquid phase. The average PO_4^{3-}-P concentration in
245 the supernatant was about 53.8 mg/L. The P in the supernatant of the fermented sludge was
246 then recovered by pH adjustment and reprecipitation. The XRD analysis (Figure S1) revealed
247 that vivianite was the main product in the recovered precipitates. With continuous sludge
248 recirculation and co-fermentation through the side stream, the overall efficiency of P recovery
249 from the wastewater influent reached an average of 61.9%.

250 The typical performance of the acidogenic sludge fermentation, including the changes of
251 pH and major chemical concentrations within three days, is shown in Figure S2. The food waste
252 (2 g-COD/L) was hydrolyzed and converted into VFAs. With acidogenesis, the VFA
253 concentration increased from 231 to 1786 mg-COD/L, leading to a decrease in pH from 5.8 to
254 4.6. Under the low pH (<5.0) condition with the VFA accumulation, methane and biogas
255 production was insignificant. In fact, very little biogas production was recorded (less than 10
256 mL/g-SS) during the 3-d acidogenic sludge fermentation. Meanwhile, ferric iron in the sludge
257 was reduced to ferrous iron by microbial iron reduction. The total Fe(II) content increased from
258 4.9 to 423.8 mg/L, which accounted for 69.6% of the total iron in the sludge. Under the acidic
259 condition, most of the ferrous iron was dissolved, releasing P, mostly orthophosphate, into the
260 supernatant.

261

262 **3.2 P speciation in the aerobic MBR and anaerobic fermenters**

263 Many possible phosphorus species exist in the Fe-dosing MBR and sludge fermentation
264 system, owing to complex reactions under both aerobic and anaerobic conditions. Wu et al.[19]
265 suggested that the main P species in Fe-dosing MBR might include ferric phosphate, ferrous

266 phosphate, phosphate adsorbed on HFO, and organic phosphorus, mainly existing as poly-
267 phosphate. Some of those chemicals would transform to mineral phases via crystallization,
268 such as strengite and vivianite. According to the XRD analysis (Figure S1), vivianite was the
269 main crystalline species found in the AnS (pH 6) and control sludge samples.

270 The acquired P K-edge XANES spectra of the reference materials are given in Figure S3.
271 Ferric phosphate (both amorphous and crystalline) and adsorbed-P had one pre-edge peak
272 around 2150 eV, which is attributable to the hybridization of Fe-3d, O-2p and P-3p orbitals.[32]
273 In the post-edge region, most of the reference compounds had one peak, while vivianite has
274 three peaks. For most of the sludge samples, the pre-edge peaks were observed, suggesting
275 ferric phosphate and/or adsorbed-P in the sludge. The spectra of AnS(pH6) and control showed
276 three peaks in the post-edge region, indicating the presence of vivianite, which is consistent
277 with the XRD result. The P K-edge XANES spectra of amorphous $FePO_4$ and strengite
278 (crystalline phase) were similar. However, crystalline $FePO_4$ was not detected by the XRD in
279 the sludge samples. Hence, the main $FePO_4$ species was apparently amorphous.

280 To identify the possible P species present in the sludge samples, PCA/TT and LCF were
281 performed on P K-edge XANES spectra. The PCA results on the ten sludge samples (Table S2)
282 suggest four principal components with a minimum indicator (IND) value of 0.0064 and a
283 cumulative variance value of 98.9%. In other words, four principal components may exist in
284 the sludge samples. Usually, the reference with a SPOIL value below 3 is considered to be
285 reasonably acceptable and the value between 3 and 6 is moderately acceptable.[33] Based on the
286 TT results (Table S3), amorphous $FePO_4$, vivianite, strengite, P-Adsorbed HFO, and phytic
287 acid were reasonably acceptable compounds selected for the LCF analysis. Based on the PCA
288 results, the combination of maximum four references was applied for LCF fitting using the
289 function of "Fit all combination", and the optimal fitting results were selected with the lowest
290 R-factor value.

The results of the XANES LCF analysis of P speciation are given in Table S4 and Figure 2a. In aerobic activated sludge from the MBR, the main P species were amorphous ferric phosphate (24.3%), adsorbed-P (60.5%), and organic-P (15.2%). During anaerobic fermentation, the P speciation and transformation were more complicated. The P speciation in the sludge mixture was determined by combining the solid P fraction data from the XANES LCF analysis and the soluble orthophosphate concentration in the supernatant (Figure 3).

Figure 3a presents the change of P species after co-fermentation. After 3 d of acidogenic fermentation, the fraction of ferric phosphate significantly decreased from 23.8% to 0%, and the fraction of adsorbed-P decreased from 59.4% to 37.9%. In contrast, the soluble orthophosphate fraction increased from 0.4% to 49.4%, whereas vivianite was barely found in the fermented sludge without pH control. Figure 3b shows the variation of P species in the fermenters under the different pH conditions. When the pH was controlled at 6, phosphorus was mainly present in the solid phase, including vivianite (39.7%), adsorbed-P (46.5%), and organic-P (7.6%). With a decreasing pH, the solid phase P species greatly decreased. When the pH decreased to 3, the soluble orthophosphate became the main P species, increasing from 6.2% to 87.4%. Figure 3c compares the P species in the fermenters under different organic loading conditions. Without the addition of food waste, soluble orthophosphate was barely observed and the main P species were adsorbed-P (57.0%), ferric phosphate (12.1%), vivianite (14.6%), and organic-P (15.3%). Compared to the activated sludge from the MBR, the fraction of adsorbed-P was not significantly decreased and the content of ferric phosphate was not greatly decreased. With food waste for co-fermentation, 49.4% of P was released from the solid phase into the solution. The residual P in the solid phase of the sludge was mainly present as adsorbed-P (37.9%) and organic-P (10.1%), whereas ferric phosphate and vivianite were barely observed.

3.3 Fe speciation in the aerobic MBR and anaerobic fermenters

Iron speciation throughout the system was more complex than that of phosphorus, due to the different valence states of ferric and ferrous iron. The solid phase of Fe(III) in activated sludge usually exists in the forms of iron (oxide-)hydroxides (ferrihydrite, goethite, akaganeite, and lepidocrocite) and strengite, and Fe(II) in the solid phase after dissimilatory iron reduction may exist as siderite, magnetite, vivianite, and ferrous hydroxides.[34] The acquired Fe K-edge XANES spectra for the various references are given in Figure S4. The absorption edge of the XANES spectra is sensitive to the oxidation state of iron in solid phase. It can be observed that the first peak position of the representative Fe(II) reference in the adsorption edge region is around 2125 eV, which is rather different from the peak of the Fe(III) reference material at around 2031 eV. The spectra of AnS(pH6) also have a peak around 2125 eV, which indicates that Fe(II) species, instead of Fe(III), were mainly present in the fermented sludge at pH 6.

PCA/TT and LCF were also performed on Fe K-edge XANES spectra to identify possible Fe species in the sludge samples. The PCA results of the ten sludge samples (Table S5) suggest four principal components with a minimum IND value of 0.00101 and a cumulative variance value of 99.8%. According to the TT results (Table S6), eight possible reference compounds can be further employed for the LCF analysis[29, 35], including three reasonably acceptable references with SPOIL values below 3 (amorphous $FePO_4$, ferrihydrite, and melanterite), and five moderately acceptable references with SPOIL values between 3 and 6 (vivianite, magnetite, lepidocrocite, siderite, and goethite). Based on the PCA results, the combination of maximum four references was applied for the LCF fitting. The results with the lowest R-factor value were selected as the optimal fitting results.

The XANES LCF analysis results of iron speciation are presented in Table S7 and Figure 2b. The species showing no presence during the fitting procedure, including melanterite, magnetite, lepidocrocite, and siderite, are not reported in the results. During fermentation,

ferrous hydroxide remained stable in the anaerobic sludge due to the low ORP (<100 mV) condition.[36] However, ferrous hydroxide can be easily oxidized in aerobic conditions.[37] When the sludge powder samples were prepared before the XANES analysis, Fe(II) hydroxide had already been transformed to Fe(III) hydroxide.[19] Thus, it was assumed in this study that the fraction of ferrihydrite detected in sludge was the sum of Fe(II) hydroxide and Fe(III) hydroxide. The iron speciation in the sludge was obtained by combining the solid-phase Fe fraction data from the XANES LCF analysis and the soluble ferrous iron content in the supernatant (Figure 4).

In the activated sludge of the Fe-dosing MBR, most of the iron was present as Fe(III), including species of ferrihydrite (52.4%), goethite (28.7%), and amorphous ferric phosphate (18.1%). During the sludge fermentation, Fe(III) was reduced and transformed to different species. Figure 4a shows that, after 3 d of fermentation, the fraction of Fe(III) hydroxide decreased significantly from 59.0% to 16.5% and that ferric phosphate completely decreased from 18.4% to 0%. In contrast, soluble ferrous iron greatly increased from 0% to 57.2% in the sludge mixture, whereas no decrease of goethite was observed. Figure 4b shows the variation of Fe species in the fermenters under the different pH conditions. At pH 6, the iron species was present mainly in the solid phase, including vivianite (54.7%), goethite (10.6%), Fe(III) hydroxide (11.8%), and Fe(II) hydroxide (6.3%). With a decrease in pH, the iron species was changed to soluble forms. When the pH was lowered to 5, vivianite was largely dissolved (from 54.7% to 1.5%). When the pH was further decreased to 3, soluble ferrous iron became the dominant species (77.9%), the remainder being goethite (7.2%) and Fe(III) hydroxide (14.8%). Figure 4c shows that, after co-fermentation with food waste, the Fe(II) fraction increased from 0.8% to 69.6%, 57.2% of the iron was dissolved as ferrous iron in the supernatant, and no ferric phosphate was observed. Without the addition of food waste, only 31.2% of the iron was reduced to ferrous iron, including vivianite (23.6%) and ferrous hydroxide (7.0%), whereas

soluble iron was barely observed at a pH of 6.3 at the end of fermentation.

4. Discussion

4.1 Fe-enhanced phosphorus removal with MBR

Smith et al.[13] proposed the following specific pathways for Fe-enhanced P removal: (i) adsorption of phosphates onto ferrihydrite, (ii) co-precipitation of phosphate species into the ferrihydrite structure, (iii) precipitation of ferric phosphate, and (iv) precipitation of mixed cation phosphates. In the present Fe-dosing MBR, more than 98% of TP was removed from the wastewater influent. According to the XANES LCF analysis, adsorbed-P formed by pathways (i) and (ii) accounted for 60.3% of TP in the sludge mixture, and ferric phosphate from pathway (iii) accounted for 24.2%. Pathway (iv) was nearly negligible owing to the high dosage of iron. The remaining P removal could be attributed to microbial assimilation for biomass growth.[38] A higher fraction of P removal could apparently be attributed to the adsorbed-P than $FePO_4$ precipitation in the Fe-dosing MBR. When $FeCl_3$ was added into wastewater, it hydrolyzed and precipitated rapidly with hydroxyl ions or phosphate ions. A solubility analysis of $Fe(OH)_3$ and $FePO_4$ in a simulated aqueous system is given in Figure S5 based on the possible reactions summarized in Table S8. Below pH 5, $FePO_4$ has the lowest relative solubility. Above pH 5, $Fe(OH)_3$ becomes more stable than $FePO_4$ and controls the solubility of Fe(III) compounds. The alkalinity of wastewater (>100 mg-$CaCO_3$/L) was sufficient to maintain the solution pH above 6 during the $FeCl_3$ dosing and flocculation. As a result, following the $FeCl_3$ addition into the wastewater influent, $Fe(OH)_3$ was the dominant iron species in the MBR sludge mixture, and adsorption by ferrihydrite was the main pathway of P removal.

Hauduc et al.[15] further suggested that the precipitation of ferrihydrite goes through three stages: (i) fresh HFO is formed initially with a very open structure and a high surface area, (ii)

390 polymerized HFO aggregates into a compact structure with less accessible binding sites, and
391 (iii) crystallized HFO, such as goethite, is formed after a long retention time. This aging and
392 compaction process leads to a reduction of HFO adsorption capacity.[39] Smith et al.[13] reported
393 a reduction of the specific HFO surface area during the aging process from 5500 m^2/g in fresh
394 HFO to 600 m^2/g in polymerized HFO. In the Fe-dosing MBR system, stage 1 took place in
395 the coagulation tank with rapid stirring, where phosphate was easily adsorbed by the sites of
396 oxygen atoms on the fresh HFO surface. This stage accounts for most of the P removal achieved
397 by the MBR. However, it was observed that 28.7% of the iron existed as goethite in the
398 activated sludge, which evidenced the transformation of ferrihydrite to goethite in the MBR
399 with a 30-d SRT. The formation of crystallized HFO could be a limiting factor for the extraction
400 of P from the sludge by biological means during fermentation. The P adsorption activity of
401 HFO is significantly affected by the pH, HFO age, and competing anions. In this study, the
402 apparent P adsorption capacity of HFO was around 0.25 g-P/g-Fe. Mao and co-workers[25]
403 reported an maximum adsorption capacity of phosphate onto fresh HFO at around 0.19 g-P/g-
404 Fe at pH 6, which is close to the experimental value in this study.
405 Wu et al.[19] reported a similar trend in the formation and speciation of Fe-based precipitates
406 (ferrihydrite and ferric phosphate) in Fe-dosing MBR system. Minor differences, however,
407 existed between the study of Wu et al. and the present results, which laid mainly in the fractions
408 and formation of lepidocrocite and goethite. Wu et al.[19] dosed $FeCl_3$ at the anoxic tank. In
409 contrast, $FeCl_3$ was quickly mixed with wastewater into the aerobic MBR in the present study.
410 The reaction conditions in the anoxic and aerobic reactors are very different that would
411 certainly affect the Fe species profile. For example, the formation of lepidocrocite requires
412 partial oxidation of Fe(II) to Fe(III), which can happen with the iron respiration in the anoxic
413 reactor under a low ORP condition, while aeration in the aerobic MBR would increase the
414 formation of goethite. The XANES-based comparison suggests the impact of Fe-dosing mode

415 on the Fe species formation during the CPR process, which can be utilized to improve the P
416 removal and recovery performance in treatment system.
417
418 **4.2 P extraction and release from sludge during acidogenic fermentation**
419 4.2.1 Acidogenic fermentation
420 A typical anaerobic digestion process includes hydrolysis, acidogenesis, and
421 methanogenesis. Acidogenic fermentation limits the digestion process to the first two steps by
422 inhibiting methanogenesis under an acidic condition (pH<5).[40] Food waste was shown to be a
423 desirable carbon source for acidogenesis because of its high biodegradability.[41] Most of the
424 organics (around 90%) in food waste could be fermented in 3 d due to the efficient hydrolysis
425 of the starch content. During co-fermentation, soluble organics acted as electron donors for
426 iron reduction.[42] Besides, a large amount of VFAs (1786 mg-COD/L) was produced through
427 acidogenesis, which decreased the solution pH to 4.85 and hence enhanced the dissolution of
428 Fe(II)-compounds. Overall, acidogenic co-fermentation in the side-stream was essential to P
429 extraction from the MBR sludge via microbial iron reduction and the dissolution of Fe-P
430 complex.
431 4.2.2 Microbial iron reduction
432 When Fe(III)-P complex in activated sludge was fed into the fermenters, microbial iron
433 reduction took place rapidly under the anaerobic condition. Without the addition of food waste
434 (control sludge), 31.7% of the total iron was transformed into Fe(II), including 23.6% vivianite
435 and 7% ferrous hydroxide, which suggests that ferrihydrite and ferric phosphate could act as
436 electron acceptors in metabolic activities.[36] However, the total Fe(III) concentration in sludge
437 was apparently too high to be substantially reduced by metabolic activities alone. With the
438 addition of food waste for co-fermentation, sufficient electron donors were provided by VFA
439 production to greatly improve the iron reduction ratio to 69.7%.
440 The fraction of Fe(III) species, including 100% of ferric phosphate, 72.1% of ferrihydrite,

and 35.9% of goethite, decreased with the ferric iron reduction. The reduction of ferric phosphate and ferrihydrite was apparently more efficient than that of goethite. The dissimilatory iron reduction kinetics was expected to be influenced by crystallinity, particle size, specific surface area, and solubility. Munch and Ottow[43] suggested that ferric compounds present in the amorphous phase, such as amorphous ferric phosphate and ferrihydrite, would be reduced preferentially over those in the crystalline phase, such as goethite. Even among the crystalline ferric phases, the reactivity of goethite towards microbial iron reduction is lower than lepidocrocite and hematite. Theoretically, reduction of goethite requires a much lower redox potential (-0.274 V) than ferrihydrite (0.014 V), whereas the redox potential in the fermenters was between -0.1 to -0.15 V. Therefore, goethite was poorly processed by the fermenters, which would affect the Fe dissolution and P release from the sludge.

4.2.3 Solubility of the Fe-P complex

After the microbial iron reduction, Fe-P complex in the fermented sludge consisted of ferric phosphate, ferrous phosphate, and phosphate adsorbed on ferrihydrite, ferrous hydroxide, and goethite. The dissolution of these Fe-P compounds was crucial for P extraction and release from the sludge. The experiment results showed an increasing trend of dissolution of the Fe-P complex when the pH decreased (Figure 3b and Figure 4b). Accordingly, phosphorus that was bound to iron or adsorbed on HFO was released as soluble orthophosphate into the supernatant. For instance, at pH 3, 87.4% of P could be released from the sludge with 77.9% of Fe dissolved.

To compare the solubility of different Fe-P species, the main equilibrium reactions involving the above chemicals under the anaerobic reactors are summarized in Table S8. Based on these reactions, the solubility of ferric phosphate, ferrous phosphate, ferrihydrite, ferrous hydroxide, and goethite as a function of the solution pH are presented in Figure S6. The results show that at a pH below 4, the solubility is in the sequence $FePO_4$ < α-FeOOH < $Fe(OH)_3$ < $Fe_3(PO_4)_2$ < $Fe(OH)_2$. Ferrous phosphate and ferrous hydroxide are much more soluble than

466 ferric phosphate, ferrihydrite, and goethite, which is consistent with the XANES findings. As
467 described in Section 4.2.2, ferric phosphate was efficiently reduced to ferrous phosphate by
468 fermentation, whereas reduction of HFO, especially goethite, could not be fully achieved. Due
469 to the low solubility of HFO, P adsorbed onto HFO was still retained in the solid phase of the
470 sludge. Therefore, the presence of residual ferrihydrite and especially goethite in the fermented
471 sludge appeared to be the limiting factor for the release of P from the solid phase of the sludge.
472 The means by which to reduce the fraction of the low-reactive HFO in the sludge for more
473 complete microbial iron reduction remains an issue for further investigation. Using low SRT
474 activated sludge or primary sludge with fresh Fe-P compounds maybe an effective way to
475 improve the overall iron reduction ratio.

476 The solubility analysis also suggests that, by using the chemical acidification methods for
477 P recovery, such as the Stuttgart process[7] and RecoPhos[8], it would require a large amount of
478 strong acids (around 0.5 g-H_2SO_4/g-SS[44]) to adjust the pH to 2 or lower to achieve a P
479 extraction results comparable to that of anaerobic sludge acidogenesis. The use of strong acids
480 is costly and dangerous. Many impurities, such as Al, Ca, Mg, and heavy metals, would be
481 dissolved from the sludge into the supernatant at the very low pH, which will affect the quality
482 of the recovered P-precipitates.[9] Moreover, the sludge after the strong chemical acidification
483 would not only be deactivated but also cause serious secondary pollution problems. Unlike
484 chemical acidification, acidogenic co-fermentation is able to release P from the sludge without
485 the use of strong acids. In this study, only 0.47 g/g-SS of food waste was added to achieve
486 around 62% P extraction from the sludge. More importantly, after acidogenic fermentation, the
487 sludge was not destroyed and can be readily returned to the MBR to maintain a long SRT for
488 biological wastewater treatment. The acidogenic co-fermentation method using low-cost food
489 waste is shown as a simple and environmentally-friendly solution for effective P recovery from
490 wastewater and sludge.

4.3 Environmental implications

The major pathways for P removal and recovery via Fe-dosing MBR and side-stream acidogenic fermentation are summarized in Figure 5. In the aerobic MBR, phosphorus in wastewater was removed by precipitation into ferric phosphate and by adsorption onto ferrihydrite. For a long SRT in the MBR, a certain portion of ferrihydrite was transformed into goethite. In the anaerobic fermenter for P release, waste organics were converted into VFAs via hydrolysis and acidogenesis to lower the solution pH. Meanwhile, organics acted as electron donors to induce microbial iron reduction. As observed in this study, ferric phosphate and ferric (oxy-)hydroxide were reduced to ferrous phosphate and ferrous hydroxide, respectively. At a lower pH, ferrous compounds dissolved, releasing soluble ferrous iron and orthophosphate into the supernatant. In summary, pH decrease and microbial iron reduction are the two critical conditions that control the dissolution of Fe-P complex and the resulting P release for recovery. Both conditions can be effectively enhanced with the addition of food waste for sludge fermentation. Eventually, with a simple pH adjustment to 8, orthophosphate and ferrous iron in the supernatant readily reprecipitated to form solid precipitates, consisting mainly of vivianite, for recovery as a raw material for P-fertilizers.

Acknowledgments

We gratefully acknowledge the funding for this research provided by grants 17204914, C7044-14G and T21-711/16R from the Research Grants Council (RGC) of the Hong Kong SAR Government, the grant KQJSCX20160226190815 from Shenzhen Municipal Science and Technology Innovation Council of Shenzhen Government, China, and the grants 51678333 and 41603093 from National Natural Science Foundation of China. The XAS beam time was granted by beamline BL16A1 at the NSRRC, Taiwan. We thank Dr. Ting-shan Chan and Mr.

Shih-Tien Tang of NSRRC for their help in the collection and analysis of spectra.

Supporting Information Available

The Supporting Information contains eight tables and six figures (Tables S1-S8 and Figures S1-S6). This material is available free of charge via the Internet at http://pubs.acs.org.

Literature Cited

(1) Yang, X. L.; Song, H. L.; Chen, M.; Cheng, B., Characterizing membrane foulants in MBR with addition of polyferric chloride to enhance phosphorus removal. *Bioresource Technology* **2011,** *102*, (20), 9490-9496.

(2) Zhang, Z. H.; Wang, Y.; Leslie, G. L.; Waite, T. D., Effect of ferric and ferrous iron addition on phosphorus removal and fouling in submerged membrane bioreactors. *Water Research* **2015,** *69*, 210-222.

(3) de-Bashan, L. E.; Bashan, Y., Recent advances in removing phosphorus from wastewater and its future use as fertilizer (1997–2003). *Water Research* **2004,** *38*, (19), 4222-4246.

(4) Schröder, J. J.; Smit, A. L.; Cordell, D.; Rosemarin, A., Improved phosphorus use efficiency in agriculture: a key requirement for its sustainable use. *Chemosphere* **2011,** *84*, (6), 822-831.

(5) BMUB New sewage sludge ordinance passed the German cabinet. http://phosphorusplatform.eu/scope-in-print/news/1395-new-sewage-sludge-ordinance-passed (15 June 2018).

(6) Yuan, Z.; Pratt, S.; Batstone, D. J., Phosphorus recovery from wastewater through microbial processes. *Current Opinion in Biotechnology* **2012,** *23*, (6), 878-883.

(7) Egle, L.; Rechberger, H.; Krampe, J.; Zessner, M., Phosphorus recovery from municipal wastewater: An integrated comparative technological, environmental and economic assessment of P recovery technologies. *Science of the Total Environment* **2016,** *571*, 522-542.

(8) Weigand, H.; Bertau, M.; Hübner, W.; Bohndick, F.; Bruckert, A., RecoPhos: Full-scale fertilizer production from sewage sludge ash. *Waste Management* **2013,** *33*, (3), 540-544.

(9) Petzet, S.; Peplinski, B.; Cornel, P., On wet chemical phosphorus recovery from sewage

546 sludge ash by acidic or alkaline leaching and an optimized combination of both. *Water*
547 *Research* **2012,** *46*, (12), 3769-3780.
548 (10) Li, R. H.; Li, B.; Li, X. Y., An integrated membrane bioreactor system with iron-dosing
549 and side-stream co-fermentation for enhanced nutrient removal and recovery: System
550 performance and microbial community analysis. *Bioresource Technology* **2018,** *260*, 248-
551 255.
552 (11) Li, R. H.; Wang, X. M.; Li, X. Y., A membrane bioreactor with iron dosing and acidogenic
553 co-fermentation for enhanced phosphorus removal and recovery in wastewater treatment.
554 *Water Research* **2018,** *129*, 402-412.
555 (12) Samie, I. F.; Römer, W., Phosphorus availability to maize plants from sewage sludge
556 treated with Fe compounds. In *Plant Nutrition: Food security and sustainability of agro-*
557 *ecosystems through basic and applied research*, Horst, W. J.; Schenk, M. K.; Bürkert, A.;
558 Claassen, N.; Flessa, H.; Frommer, W. B.; Goldbach, H.; Olfs, H. W.; Römheld, V.;
559 Sattelmacher, B.; Schmidhalter, U.; Schubert, S.; v. Wirén, N.; Wittenmayer, L., Eds.
560 Springer Netherlands: Dordrecht, 2001; pp 846-847.
561 (13) Smith, S.; Takacs, I.; Murthy, S.; Daigger, G. T.; Szabo, A., Phosphate complexation
562 model and its implications for chemical phosphorus removal. *Water Environment*
563 *Research* **2008,** *80*, (5), 428-438.
564 (14) Thistleton, J.; Berry, T.-A.; Pearce, P.; Parsons, S., Mechanisms of chemical phosphorus
565 removal II: Iron (III) salts. *Process Safety and Environmental Protection* **2002,** *80*, (5),
566 265-269.
567 (15) Hauduc, H.; Takács, I.; Smith, S.; Szabo, A.; Murthy, S.; Daigger, G. T.; Spérandio, M.,
568 A dynamic physicochemical model for chemical phosphorus removal. *Water Research*
569 **2015,** *73*, 157-170.
570 (16) Rasmussen, H.; Nielsen, P. H., Iron reduction in activated sludge measured with different
571 extraction techniques. *Water Research* **1996,** *30*, (3), 551-558.
572 (17) Gu, S.; Qian, Y.; Jiao, Y.; Li, Q.; Pinay, G.; Gruau, G., An innovative approach for
573 sequential extraction of phosphorus in sediments: Ferrous iron P as an independent P
574 fraction. *Water Research* **2016,** *103*, 352-361.
575 (18) Cui, J. L.; Luo, C. L.; Tang, C. W. Y.; Chan, T. S.; Li, X. D., Speciation and leaching of
576 trace metal contaminants from e-waste contaminated soils. *Journal of Hazardous*
577 *Materials* **2017,** *329*, 150-158.
578 (19) Wu, H.; Ikeda Ohno, A.; Wang, Y.; Waite, T. D., Iron and phosphorus speciation in Fe-
579 conditioned membrane bioreactor activated sludge. *Water Research* **2015,** *76*, 213-226.

(20) Kim, H.; Kim, J.; Shin, S. G.; Hwang, S.; Lee, C., Continuous fermentation of food waste leachate for the production of volatile fatty acids and potential as a denitrification carbon source. *Bioresource Technology* **2016,** *207*, 440-445.

(21) Cornell, R. M.; Schwertmann, U., *The Iron Oxides: Structure, Properties, Reactions, Occurrences and Uses*, ed. Wiley: New York, 2003.

(22) Reinsch, B. C.; Forsberg, B.; Penn, R. L.; Kim, C. S.; Lowry, G. V., Chemical transformations during aging of zerovalent iron nanoparticles in the presence of common groundwater dissolved constituents. *Environmental Science & Technology* **2010,** *44*, (9), 3455-3461.

(23) Dalas, E., The crystallization of ferric phosphate on cellulose. *Journal of Crystal Growth* **1991,** *113*, (1-2), 140-146.

(24) Mattievich, E.; Danon, J., Hydrothermal synthesis and Mössbauer studies of ferrous phosphates of the homologous series Fe3 2+(PO4)2(H2O)n. *Journal of Inorganic and Nuclear Chemistry* **1977,** *39*, (4), 569-580.

(25) Mao, Y.; Ninh Pham, A.; Xin, Y.; David Waite, T., Effects of pH, floc age and organic compounds on the removal of phosphate by pre-polymerized hydrous ferric oxides. *Separation and Purification Technology* **2012,** *91*, 38-45.

(26) Ravel, B.; Newville, M., ATHENA, ARTEMIS, HEPHAESTUS: data analysis for X-ray absorption spectroscopy using IFEFFIT. *Journal of Synchrotron Radiation* **2005,** *12*, 537-541.

(27) Ressler, T.; Wong, J.; Roos, J.; Smith, I. L., Quantitative speciation of Mn-bearing particulates emitted from autos burning (methylcyclopentadienyl) manganese tricarbonyl-added gasolines using XANES spectroscopy. *Environmental Science & Technology* **2000,** *34*, (6), 950-958.

(28) Webb, S. M., SIXpack: a graphical user interface for XAS analysis using IFEFFIT. *Physica Scripta* **2005,** *2005*, (T115), 1011.

(29) Zhao, Y.-p.; Cui, J.-l.; Chan, T.-s.; Dong, J.-c.; Chen, D.-l.; Li, X.-d., Role of chelant on Cu distribution and speciation in Lolium multiflorum by synchrotron techniques. *Science of the Total Environment* **2018,** *621*, 772-781.

(30) APHA, *Standard Methods for Examination of Water and Wastewater*, 22nd ed. American Public Health Association, American Water Work Association, Water Environment Federation: Washington DC, 1998.

(31) Wang, X. M.; Waite, T. D., Iron speciation and iron species transformation in activated sludge membrane bioreactors. *Water Research* **2010,** *44*, (11), 3511-3521.

(32) Xiong, W.; Peng, J.; Hu, Y., Use of X-ray absorption near edge structure (XANES) to identify physisorption and chemisorption of phosphate onto ferrihydrite-modified diatomite. *Journal of Colloid and Interface Science* **2012,** *368*, (1), 528-532.
(33) Malinowski, E. R., *Factor analysis in chemistry*, 3rd ed. Wiley: New York, 2002.
(34) Zachara, J. M.; Kukkadapu, R. K.; Fredrickson, J. K.; Gorby, Y. A.; Smith, S. C., Biomineralization of poorly crystalline Fe (III) oxides by dissimilatory metal reducing bacteria (DMRB). *Geomicrobiology Journal* **2002,** *19*, (2), 179-207.
(35) Cui, J.; Jing, C.; Che, D.; Zhang, J.; Duan, S., Groundwater arsenic removal by coagulation using ferric(III) sulfate and polyferric sulfate: A comparative and mechanistic study. *Journal of Environmental Sciences* **2015,** *32*, 42-53.
(36) Weber, K. A.; Achenbach, L. A.; Coates, J. D., Microorganisms pumping iron: anaerobic microbial iron oxidation and reduction. *Nature Reviews: Microbiology* **2006,** *4*, (10), 752-764.
(37) Ruby, C.; Abdelmoula, M.; Naille, S.; Renard, A.; Khare, V.; Ona-Nguema, G.; Morin, G.; Genin, J. M. R., Oxidation modes and thermodynamics of FeII-III oxyhydroxycarbonate green rust: Dissolution-precipitation versus in situ deprotonation. *Geochimica et Cosmochimica Acta* **2010,** *74*, (3), 953-966.
(38) Lee, J. K.; Choi, C. K.; Lee, K. H.; Yim, S. B., Mass balance of nitrogen, and estimates of COD, nitrogen and phosphorus used in microbial synthesis as a function of sludge retention time in a sequencing batch reactor system. *Bioresource Technology* **2008,** *99*, (16), 7788-7796.
(39) Bligh, M. W.; Waite, T. D., Formation, aggregation and reactivity of amorphous ferric oxyhydroxides on dissociation of Fe(III)-organic complexes in dilute aqueous suspensions. *Geochimica et Cosmochimica Acta* **2010,** *74*, (20), 5746-5762.
(40) Appels, L.; Baeyens, J.; Degrève, J.; Dewil, R., Principles and potential of the anaerobic digestion of waste-activated sludge. *Progress in Energy and Combustion Science* **2008,** *34*, (6), 755-781.
(41) Shen, D. S.; Yin, J.; Yu, X. Q.; Wang, M. Z.; Long, Y. Y.; Shentu, J.; Chen, T., Acidogenic fermentation characteristics of different types of protein-rich substrates in food waste to produce volatile fatty acids. *Bioresource Technology* **2017,** *227*, 125-132.
(42) Finke, N.; Vandieken, V.; Jorgensen, B. B., Acetate, lactate, propionate, and isobutyrate as electron donors for iron and sulfate reduction in Arctic marine sediments, Svalbard. *FEMS Microbiology Ecology* **2007,** *59*, (1), 10-22.
(43) Munch, J. C.; Ottow, J. C. G., Reductive transformation mechanism of ferric oxides in

hydromorphic soils. *Ecological Bulletins* **1983**, (35), 383-394.

(44) Franz, M., Phosphate fertilizer from sewage sludge ash (SSA). *Waste Management* **2008,** *28*, (10), 1809-1818.

Figure captions

Figure 1. Schematics of the chemical-biological wastewater treatment system for enhanced P removal and recovery, including Fe-dosing, aerobic MBR, and side-stream sludge co-fermentation.

Figure 2. (a) P and (b) Fe K-edge XANES analysis of the sludge samples, with symbols representing the XANES spectrum data and lines from the linear combination fitting.

Figure 3. P speciation characterized by the chemical measurements and XANES analysis on the sludge samples as a function of the (a) fermentation period, (b) pH, and (c) organic loading. Soluble P (SP) was determined by the ascorbic acid reduction method.[30]

Figure 4. Fe speciation characterized by the chemical measurements and XANES analysis on the sludge samples as a function of the (a) fermentation period, (b) pH, and (c) organic loading. Soluble Fe(II) (SFe(II)) was determined by the phenanthroline method.[30]

Figure 5. Major reactions and transformations involved in P removal and recovery throughout the various stages of the wastewater treatment and P recovery system.

Table 1. Sludge samples obtained from the different batch fermentation conditions for the XANES analysis.

No.	Reactor	Sample	Fermentation time (h)	pH	Organic loading (g-COD/L)
1	I	AnS(T0)	0	No control	2
2	I	AnS(T24)	24	No control	2
3	I	AnS(T48)	48	No control	2
4	I	AnS(T72)	72	No control	2
5	II	AnS(pH3)	72	3	2
6	III	AnS(pH4)	72	4	2
7	IV	AnS(pH5)	72	5	2
8	V	AnS(pH6)	72	6	2
9	VI	Control	72	No control	0

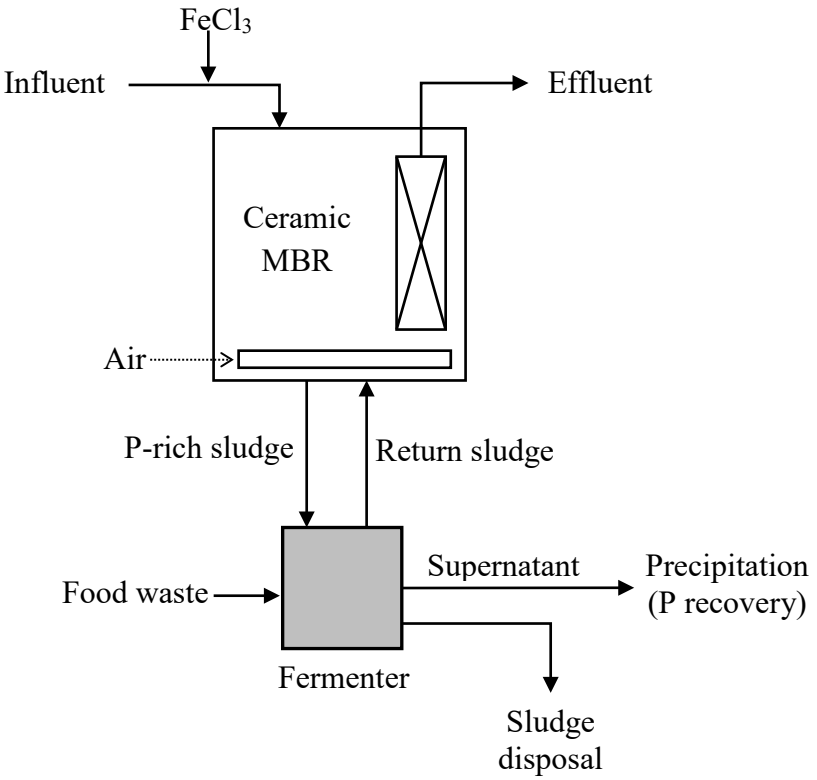

Figure 1. Schematics of the chemical-biological wastewater treatment system for enhanced P removal and recovery, including Fe-dosing, aerobic MBR, and side-stream sludge co-fermentation.

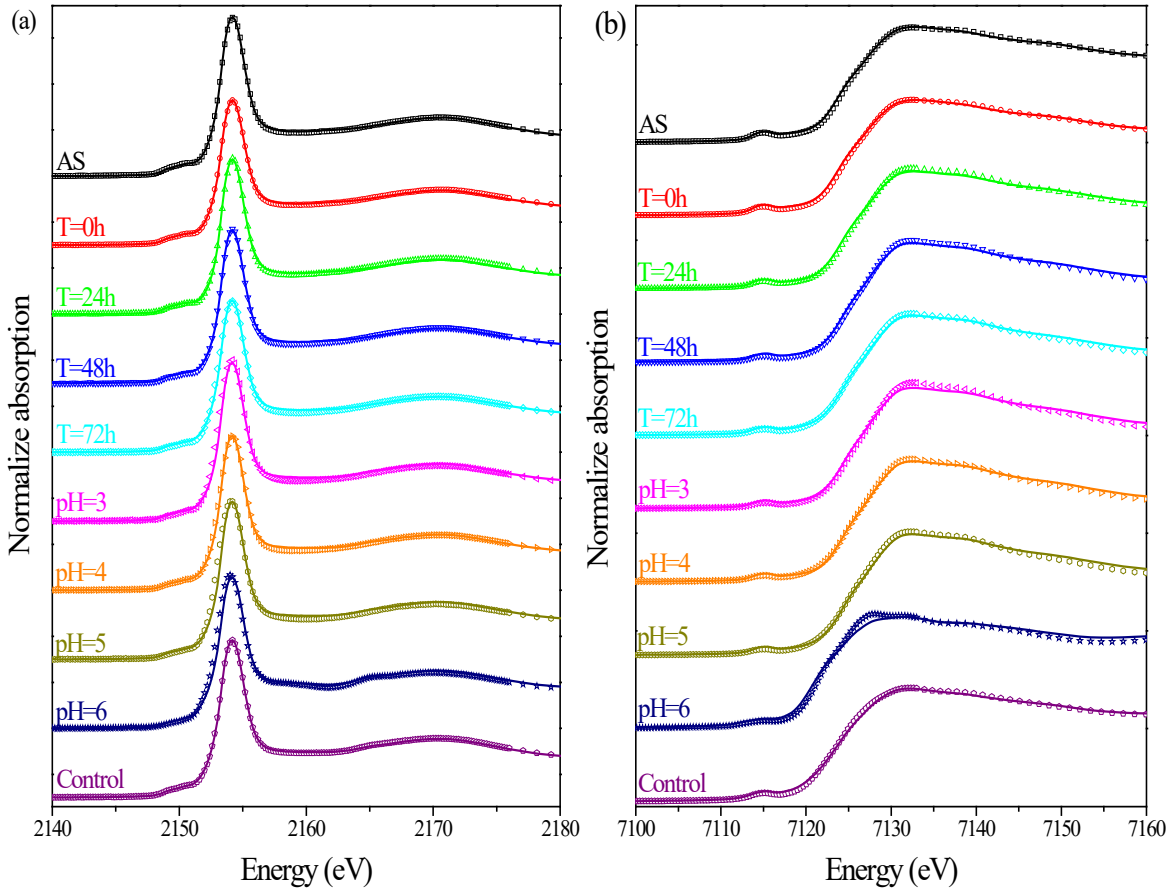

Figure 2. (a) P and (b) Fe K-edge XANES analysis of the sludge samples, with symbols representing the XANES spectrum data and lines from the linear combination fitting.

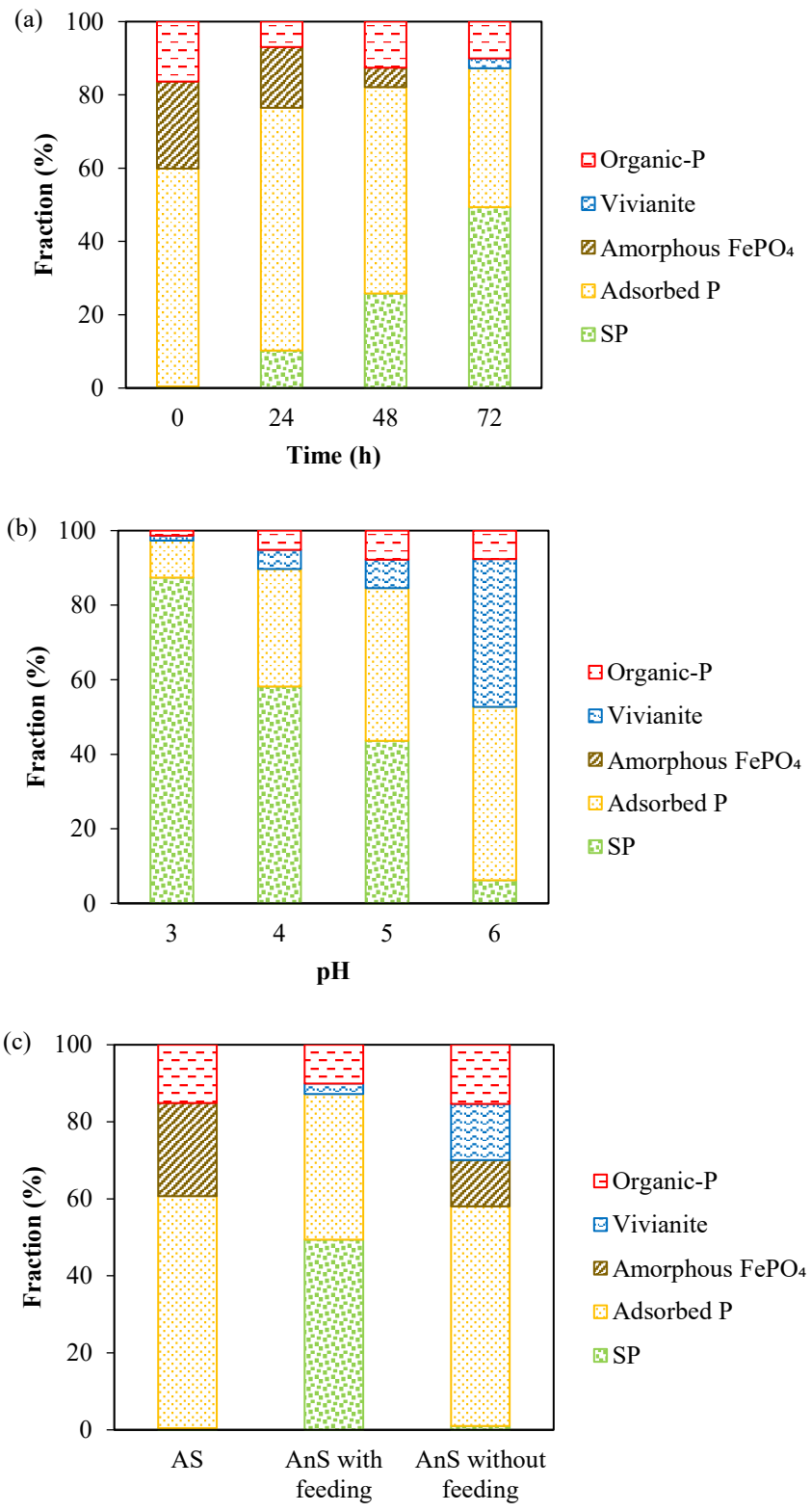

Figure 3. P speciation characterized by the chemical measurements and XANES analysis on the sludge samples as a function of the (a) fermentation period, (b) pH, and (c) organic loading. Soluble P (SP) was determined by the ascorbic acid reduction method.[30]

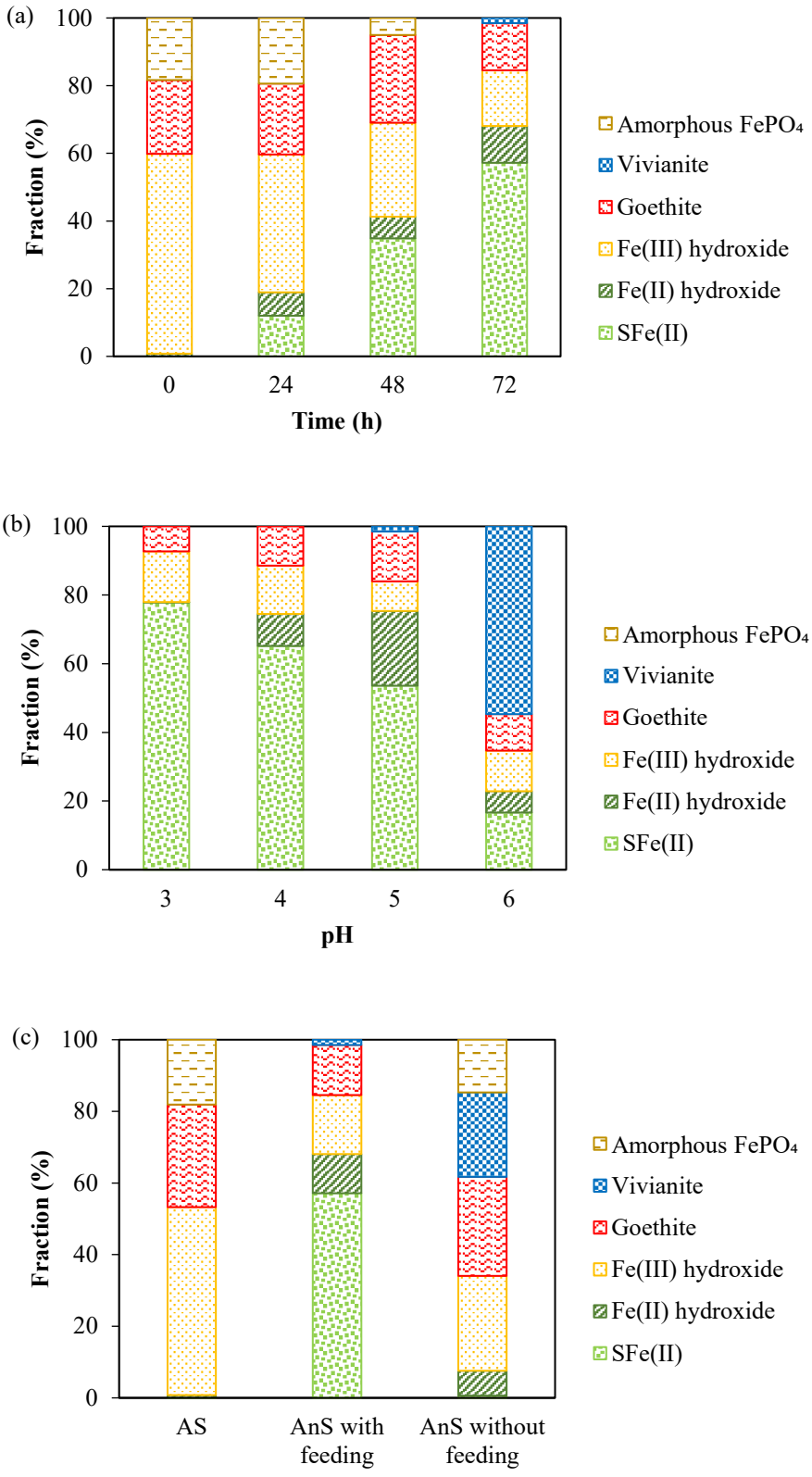

Figure 4. Fe speciation characterized by the chemical measurements and XANES analysis on the sludge samples as a function of the (a) fermentation period, (b) pH, and (c) organic loading. Soluble Fe(II) (SFe(II)) was determined by the phenanthroline method.[30]

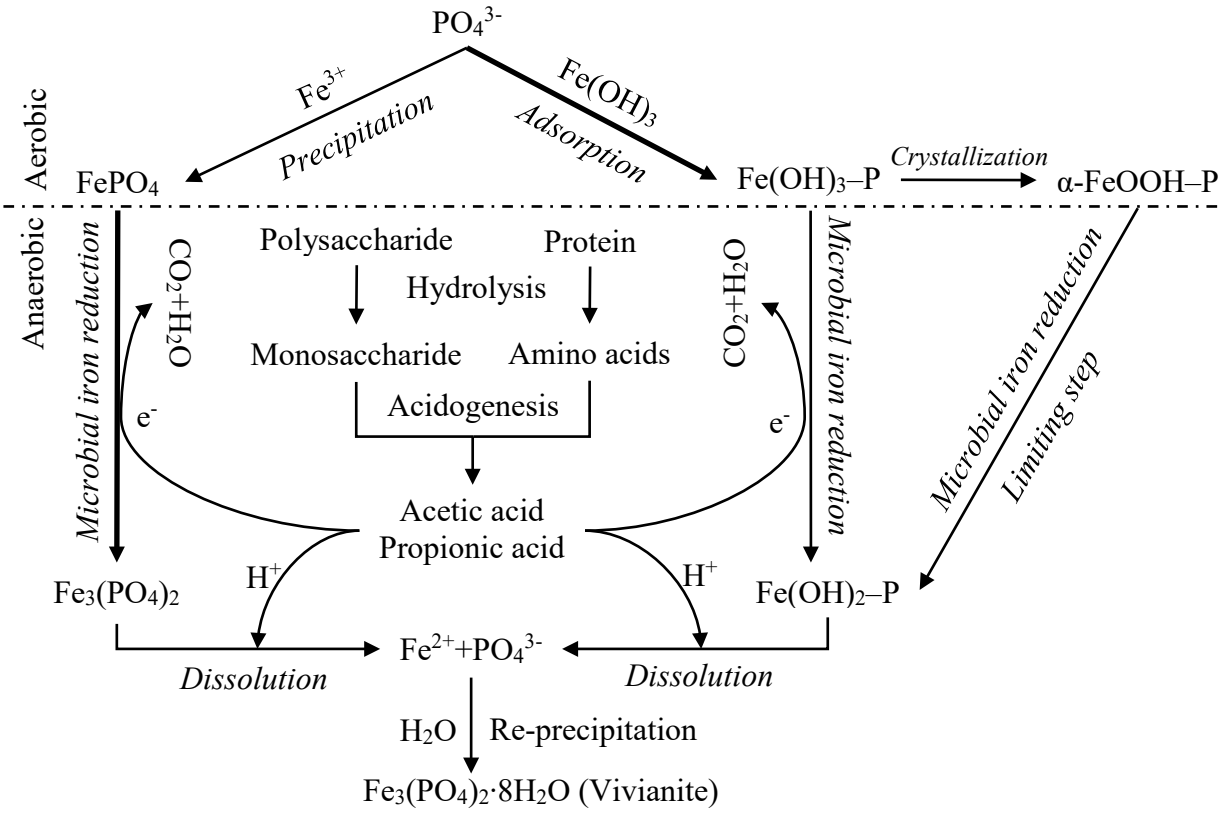

Figure 5. Major reactions and transformations involved in P removal and recovery throughout the various stages of the wastewater treatment and P recovery system.